An investigation of coupled energy and particle transport in tokamak plasmas

N Deliyanakis†, C M Bishop, J W Connor, M Cox and D C Robinson

UKAEA/Euratom Fusion Association, Culham Laboratory, Abingdon, Oxfordshire
OX14 3DB, UK

Abstract. This paper examines some experimental evidence for coupling between particle and energy transport in tokamak plasmas and presents analytical and numerical investigations of this type of transport. This coupling generally leads to discrepancies between the effective thermal diffusivities inferred from analyses of power balance and perturbation measurements. Such discrepancies have been observed experimentally. Comparisons are presented between the results from the numerical solution of a coupled transport model and data from experiments with modulated heating carried out on the DITE machine. The salient features of coupled transport have been assessed and demonstrated to be fully consistent with experimental data: it has been shown that transport matrices with relatively large off-diagonal components can lead to small apparent perturbations of the density, when the energy balance is perturbed, whilst still affecting the thermal transport considerably. Furthermore, perturbation measurements, used in conjunction with *predictive* transport codes, have emerged as a useful technique for validating transport models.

1. Introduction and overview

Present methods of interpreting tokamak transport are often incompatible with the complications postulated by theoretical transport models. The assumptions usually made when analysing thermal transport by equilibrium (power balance) and dynamical (perturbation) techniques are that the thermal flux is driven solely by a temperature gradient and that the thermal diffusivity is a function of radius rather than a function of the plasma parameters and their gradients. However, most theoretical models predict particle and energy fluxes that are each driven by both density and temperature gradients, leading to coupling; moreover, the corresponding transport coefficients are often predicted to be complex functions of the gradients or of other plasma parameters (thus leading to *intrinsic* coupling). One notes that

(i) an *effective* thermal diffusivity can be defined for any transport model, no matter how complicated, i.e.

$$\chi_{\text{eff}} = -q/nT' \tag{1}$$

where q is the thermal flux and T' is the temperature gradient (the corresponding perturbed quantities are used in a dynamical measurement);

† Present address: JET Joint Undertaking, Abingdon, Oxfordshire OX14 3EA, UK.

(ii) the value of this effective diffusivity will generally depend on the measurement technique as well as on the underlying fluxes, discrepancies between such diffusivities having been observed experimentally; and

(iii) a perturbation of the energy balance can change the density profile, even when the particle source does not change.

It has been pointed out by Hossain *et al* (1987) that, in the presence of coupling between particle and energy transport, the temperature is not an eigenfunction of the coupled system of partial differential equations nor is the thermal conductivity an eigenvalue. Further discrepancies can arise when the transport coefficients are functions of the perturbed variables and their gradients, as shown by Gentle (1988). A thermal pinch may also be present and, in practice, it may be difficult to distinguish between the effects of such a contribution to the thermal flux and one due to diffusive terms. Measurements of the thermal diffusivity that have been carried out in the past on several tokamaks (Fredrickson *et al* 1986, Tubbing *et al* 1987, Jahns *et al* 1986, Gambier *et al* 1990) typically lead to estimates inferred from dynamical techniques (corresponding to 'incremental' diffusivities) that are higher than those obtained from power-balance analyses. The question therefore arises as to whether coupled transport can explain the experimental observations and whether particular transport models are compatible with experimental results.

This paper investigates the causes and effects of coupled transport with consideration of relevant experimental observations. Analytical solutions of a simplified case of coupled transport have confirmed the presence of the effects discussed above, which can also arise through parametric dependences of the relevant transport coefficients on perturbed variables. The results of this analysis suggest that it is possible conclusively to test proposed transport models on the basis of results from different measurements of transport, using the well-established techniques based on power balance and the propagation of the heat pulses associated with the sawtooth collapse and modulated, localized heating, in conjunction with *predictive* (or inductive) rather than direct (or deductive) interpretation.

A predictive, numerical model of coupled transport has been developed and applied, taking into account several, but not all, possible complications. This model has produced results that are fully consistent with experimental data from transport measurements carried out on the DITE tokamak (Ashraf *et al* 1988, Cox *et al* 1993, Deliyanakis 1989), supporting the presence of coupled transport. Although these data have also been interpreted on the basis of a simple thermal diffusion model, as reported in the references above, the evidence for coupled transport remains strong. A discrepancy between the effective thermal diffusivities from power balance and modulated heating has been reproduced, and a local density modulation, which is significantly reduced upon chordal integration, has been predicted. Section 2 presents and discusses the experimental evidence for coupled transport. Section 3 contains a simplified, analytical treatment of the underlying problem. Section 4 describes the detailed, numerical approach to the problem, based on predictive modelling, whilst in section 5 the results of the numerical analysis are compared with experimental data from the DITE tokamak. In section 6 conclusions are drawn and recommendations for further investigations are made.

2. Experimental background and indications of coupled transport

The present investigation into coupled transport is based on the results from the experiments with modulated electron cyclotron resonance heating (ECRH) carried out on the DITE tokamak; these are presented in detail by Ashraf *et al* (1988), Cox *et al* (1993) and

Deliyanakis (1989). The two important features of these experimental results in relation to the issue of coupled transport were as follows.

(i) The line-averaged density exhibited a small modulation during the modulation of the ECRH power. The modulation level of the central chord signal was about 0.2–0.5% for fundamental resonance heating and about 1.5% for second harmonic resonance heating (with a lower plasma current, at lower densities), to be compared with the modulation level of the central temperature (ECE) signal, of 5–12%. The density modulation level was lower for helium plasmas than for hydrogen/deuterium plasmas, particularly for chords nearer the edge (see Cox *et al* 1993). On all chords, the density was observed initially to *decrease* from its equilibrium level, at the time when the (positive) energy perturbation was applied, before starting to oscillate.

(ii) The values inferred for the effective electron thermal diffusivity χ_{eff} from the thermal transport analysis of the modulation results and from parallel analyses of power balance and sawtooth heat pulse propagation were in good agreement and showed the expected reciprocal scaling with line-averaged density (reflecting the linear scaling of the energy confinement time with density). This result, however, was dependent upon the use of ECRH absorption profiles calculated by a ray-tracing code, which predicted broad profiles for high densities: previous estimates based on narrower profiles indicated that, at higher densities, the thermal diffusivity from modulation was higher than the corresponding values from the two other techniques (Cox *et al* 1993, Deliyanakis 1989). Similar experiments on other tokamak devices have often, albeit not universally, resulted in discrepancies between the thermal diffusivity values from dynamical and equilibrium measurements, the former yielding higher values than the latter (Fredrickson *et al* 1986, Tubbing *et al* 1987, Jahns *et al* 1986, Gambier *et al* 1990).

There are three distinct mechanisms that can give rise to a modulation of the observed line-integrated density in a discharge with modulated heating; the interaction of these mechanisms may produce either a reinforcement or a cancellation of the modulation:

(i) Off-diagonal diffusivities in the linearized energy and particle balance equations will lead to coupling between the particle and energy balance. (In general, this coupling involves both electron and ion energy transport as well as the current density evolution.) This will result in a density perturbation and will, at the same time, lead to different values for the thermal diffusivity being inferred from dynamical and equilibrium measurements.

(ii) The particle source will be modulated, because of the direct absorption of the ECRH wave at the edge, the interaction of the propagating thermal wave at the edge and the modulated plasma column shift. This effect has been observed in the Hα-radiation signals, which exhibit a prompt response attributed to the direct absorption, and a delayed response attributed to the thermal wave interaction. Recycling is expected to reduce the density modulation; as recycling is stronger in helium than in hydrogen/deuterium plasmas, this may contribute to the differences between the observed density modulation levels.

(iii) The modulation of the plasma pressure will produce a modulated, horizontal movement of the flux surfaces, leading to a modulation of the observed line-integrated density (as well as to similar contributions to the soft x-ray signals from vertical viewing lines and the ECE signals).

3. Analytical investigation of coupled transport

Insight into the nature and effects of transport coupling mechanisms, and the way in which discrepancies can arise between the effective diffusivities obtained from equilibrium and

dynamical measurements, can be gained with the help of analytical solutions of a simplified problem. Here, the treatment presented by Bishop and Connor (1990) has been elucidated and extended to cover the sawtooth collapse in addition to modulated heating.

The following coupled equations describing particle and energy transport are taken as the basis of this analysis, where the assumption of a single radial dependence for all the diffusivities is made, pinch terms are incorporated in the source terms, and the convective contribution of the particle flux to the thermal flux has been explicitly included:

$$\frac{\partial n}{\partial t} = \frac{1}{r}\frac{\partial}{\partial r}\left[rnf(r)\left(L_{11}\frac{n'}{n} + L_{12}\frac{T'}{T}\right)\right] + S(r,t) \tag{2}$$

$$\frac{\partial(\frac{3}{2}nT)}{\partial t} = \frac{1}{r}\frac{\partial}{\partial r}\left[rnTf(r)\left((L_{21} + \tfrac{5}{2}L_{11})\frac{n'}{n} + (L_{22} + \tfrac{5}{2}L_{12})\frac{T'}{T}\right)\right] + Q(r,t). \tag{3}$$

Analytical progress is possible after linearizing and simplifying these equations by assuming small perturbations of small scale-lengths, such that $n\tilde{n}' \gg n'\tilde{n}$ and $T\tilde{T}' \gg T'\tilde{T}$, yielding

$$\frac{\partial}{\partial t}\begin{pmatrix}\tilde{n}/n \\ \tilde{T}/T\end{pmatrix} = \frac{1}{r}\frac{\partial}{\partial r}\left\{[rf(r)\mathbf{M}]\cdot\frac{\partial}{\partial r}\begin{pmatrix}\tilde{n}/n \\ \tilde{T}/T\end{pmatrix}\right\} + \begin{pmatrix}\tilde{S}/n \\ \tfrac{2}{3}\tilde{Q}/nT - \tilde{S}/n\end{pmatrix} \tag{4}$$

where the elements of the dynamical diffusivity matrix $\mathbf{M}$ are:

$$M_{11} = L_{11} \qquad M_{12} = L_{12} \qquad M_{21} = \tfrac{2}{3}(L_{21} + L_{11}) \qquad M_{22} = \tfrac{2}{3}(L_{22} + L_{12}). \tag{5}$$

The right-hand side of these equations would, in general, include first-order terms arising from particle and energy pinches, as well as the zeroth-order terms arising from perturbed sources and fluxes; these effects have been omitted here for they do not change the nature of the solutions, but they will be included in the numerical analysis. The linearized system of equations can be solved by diagonalizing the diffusivity matrix $\mathbf{M}$, leading to the decoupled diffusion equations; in the region where the source perturbations are nil†, one obtains

$$\frac{\partial\xi_\pm}{\partial t} = \frac{1}{r}\frac{\partial}{\partial r}\left[rf(r)\lambda_\pm\frac{\partial\xi_\pm}{\partial r}\right] \tag{6}$$

where the eigenvalues λ_+ and λ_- of the diffusivity matrix are the diffusivities of the eigenfunctions $\xi_+(r,t)$ and $\xi_-(r,t)$ respectively. The coupled solutions for the density and temperature perturbations are related to the eigenfunctions by the transformation

$$\begin{pmatrix}\tilde{n}/n \\ \tilde{T}/T\end{pmatrix} = \begin{pmatrix}1 & 1 \\ u_+ & u_-\end{pmatrix}\begin{pmatrix}\xi_+ \\ \xi_-\end{pmatrix} \tag{7}$$

and the eigenvalues and corresponding eigenvector components are given by

$$\lambda_\pm = \tfrac{1}{2}\{(M_{11} + M_{22}) \pm [(M_{11} - M_{22})^2 + 4M_{12}M_{21}]^{1/2}\} \qquad u_\pm = \frac{\lambda_\pm - M_{11}}{M_{12}}. \tag{8}$$

---

† The reader can readily generalize the solutions given here for a case with non-vanishing sources, by using the inverse transformation matrix $\mathbf{U}^{-1}$ to transform the source vector in the right-hand side of (4) to a source vector for the decoupled system (6) (see, e.g., O'Rourke 1993).

It can be seen that the original diffusion coefficients are not eigenvalues of the system nor are the density and temperature its eigenfunctions. For a flat profile $f(r)$, the solutions of (6) are given in terms of Bessel functions (see, e.g., Cox *et al* 1993). For clarity, we assume infinite slab geometry for the remainder of this analytical investigation, so that (6) becomes

$$\frac{\partial \xi_\pm}{\partial t} = \lambda_\pm \frac{\partial^2 \xi_\pm}{\partial x^2}. \tag{9}$$

Assuming a perturbation of angular frequency ω, the eigenfunctions (for $x \geqslant 0$) are

$$\xi_\pm(x,t) = \exp(-s_\pm x)[A_\pm \cos(\omega t - s_\pm x) + B_\pm \sin(\omega t - s_\pm x)] \tag{10}$$

with

$$s_\pm = \left(\frac{\omega}{2\lambda_\pm}\right)^{1/2}. \tag{11}$$

(The amplitudes $A_\pm$ and $B_\pm$ with which the eigenmodes are excited depend on the source perturbations.)

We first consider the problem of the density and temperature responses to modulated ECRH and we introduce a modulated, localized excitation of the energy balance at $x=0$, i.e. $\tilde{S} = 0$ and $\tilde{Q} = P\delta(x)\cos(\omega t)$. From the null particle flux perturbation at $x = 0$, i.e.

$$\left(M_{11}\left(\frac{\tilde{n}}{n}\right)' + M_{12}\left(\frac{\tilde{T}}{T}\right)'\right)\Bigg|_{x=0} = 0 \tag{12}$$

we obtain an eigenmode ratio

$$\frac{A_+}{A_-} = \frac{B_+}{B_-} = -\frac{s_-(M_{11} + M_{12}u_-)}{s_+(M_{11} + M_{12}u_+)} = -\left(\frac{\lambda_-}{\lambda_+}\right)^{1/2}. \tag{13}$$

(The absolute amplitudes can be determined from the finite thermal flux perturbation.) It is important to note that a different perturbation will generally lead to a different combination of eigenmodes, and thereby to different density and temperature perturbations, associated with a distinct effective diffusivity. We therefore consider, as an illustration, the perturbations associated with the sawtooth collapse: as this involves a rapid flattening of the equilibrium profiles within the mixing radius, we assume that the density and temperature perturbations are excited simultaneously at $x = 0$, with amplitudes in the ratio of the density and temperature gradients, i.e.

$$\left(\frac{\tilde{T}}{T}\right) \bigg/ \left(\frac{\tilde{n}}{n}\right)\Bigg|_{x=0} = \frac{T'/T}{n'/n} = \eta \tag{14}$$

we now obtain an eigenmode ratio

$$\frac{A_+}{A_-} = \frac{B_+}{B_-} = -\frac{\eta - u_-}{\eta - u_+}. \tag{15}$$

From (13) and (15) it follows that, for the perturbations considered, the two eigenmodes, and therefore the density and temperature perturbations, have the same phase at $x = 0$. The

'near-field' solution, for $x \to 0$, gives a ratio of density and temperature relative modulation amplitudes

$$\frac{|\tilde{n}/n|}{|\tilde{T}/T|} = \left| \frac{(A_+/A_-) + 1}{u_+(A_+/A_-) + u_-} \right| \tag{16}$$

which depends on the form of the perturbation; the 'far-field' solution, for $x \to \infty$, is dominated by the eigenfunction with the larger eigenvalue λ_+ and gives a ratio

$$\frac{|\tilde{n}/n|}{|\tilde{T}/T|} = \left| \frac{1}{u_+} \right|. \tag{17}$$

We now address the problem of the discrepancy between the effective thermal diffusivities that are obtained from analyses of the perturbed system described by (4) and from measurements on the equilibrium solutions of (2) and (3). In the dynamical case, one measures the perturbed thermal flux $\tilde{q} = -n\chi^{HP}\tilde{T}'$. The phase of the temperature perturbation $(\tilde{T}/T)$ is

$$\phi_{\tilde{T}} = -\frac{\pi}{4} - \tan^{-1}\left[\frac{u_+A_+ \exp(-s_+x)\sin(s_+x) + u_-A_- \exp(-s_-x)\sin(s_-x)}{u_+A_+ \exp(-s_+x)\cos(s_+x) + u_-A_- \exp(-s_-x)\cos(s_-x)} \right]. \tag{18}$$

The relevant effective diffusivity $\frac{2}{3}\chi_{eff}^{HP}$, as this would be measured from the spatially varying heat pulse phase, is related to the phase gradient, $s_{eff} = -\phi'_{\tilde{T}}$, by an equation of the same form as (11). Hence, in the 'near-field' limit $x \to 0$, we obtain

$$\chi_{eff}^{HP} = \frac{3}{2} \left(\frac{u_+(A_+/A_-)\lambda_+^{-1/2} + u_-\lambda_-^{-1/2}}{u_+(A_+/A_-) + u_-} \right)^{-2} \tag{19}$$

in the 'far-field' limit $x \to \infty$, we obtain

$$\chi_{eff}^{HP} = \frac{3}{2}\lambda_+. \tag{20}$$

(Note that a different result would have been obtained from the amplitude decay length.) In the equilibrium case, one measures the steady-state thermal flux $q = -n\chi^{PB}T'$; the relevant thermal diffusivity χ_{eff}^{PB} is a linear combination of the two energy diffusivities L_{21} and L_{22} in the equilibrium energy balance equation, that is

$$\chi_{eff}^{PB} = L_{21}\eta^{-1} + L_{22} \tag{21}$$

where the profile parameter $\eta = (T'/T)/(n'/n)$ is a characteristic of the equilibrium solution.

Most theories of transport predict dependences of the transport coefficients on the local plasma parameters from which the observed radial dependences arise. However, in the presence of a perturbation, these dependences will lead to corresponding perturbations in the transport coefficients and to a modification of the behaviour that would have been observed with constant coefficients. In a linearized perturbation approximation, a perturbed transport coefficient will produce an effect by acting on the corresponding equilibrium gradient, thus leading to modified or even new dynamical coefficients. As an illustration of

these effects, we now consider a case where all the diffusivities of the equilibrium system have a dependence on, say, the density gradient. We take a particle flux

$$\Gamma = -nf(r)\left(\frac{n'}{n}\right)^{\ell}\left(L_{11}\frac{n'}{n} + L_{12}\frac{T'}{T}\right) \tag{22}$$

the linearized perturbed particle flux, obtained after a Taylor expansion and some algebraic manipulation (with the same assumptions as those used for the linearization of the transport equations), is

$$\tilde{\Gamma} = -nf(r)\left(\frac{n'}{n}\right)^{\ell}\left[((\ell+1)L_{11} + \ell\eta L_{12})\left(\frac{\tilde{n}}{n}\right)' + L_{12}\left(\frac{\tilde{T}}{T}\right)'\right] \tag{23}$$

with a similar result for the thermal flux; one notes that the perturbed diffusivities now depend on the equilibrium solutions through the parameter η. The subsequent treatment proceeds in the same way as above, the expressions for the dynamical diffusivities in (5) being modified, using the substitutions $L_{11}\rightarrow(\ell+1)L_{11}+\ell\eta L_{12}$ and $L_{21}\rightarrow(\ell+1)L_{21}+\ell\eta L_{22}$.

The effects of coupling have been investigated for three transport models, namely the collisionless and collisional neoclassical models (Hinton and Hazeltine 1976), and the anomalous dissipative-trapped-electron (DTE) mode (Horton 1976), one of the plausible candidates for anomalous transport; the latter predicts diffusivities with a cubic dependence on the density gradient, that is with $\ell = 3$ in the treatment above. The different perturbations and effective thermal diffusivities were evaluated for these models, for the typical profile parameter $\eta = 1.5$; the results are shown in table 1 and are broadly consistent with the experimental observations discussed in section 2; in particular, the *dynamical* values of the effective thermal diffusivity are *higher* than the corresponding *equilibrium* values, and the density perturbations are typically smaller in relative amplitude than the temperature perturbations. However, the results obtained for the DTE mode indicate exceptionally large discrepancies that are not consistent with experimental observations. It should finally be noted that the parameters considered in this analysis depend only on the *relative* magnitudes of the transport coefficients.

Table 1. Results from analytical investigation of coupled transport systems: *relative* magnitudes of steady-state transport coefficients; ratio of density to temperature perturbations, and ratio of effective thermal diffusivities from heat pulse and power balance measurements, based on heating modulation (mod) and sawtooth (s/t) heat pulses (profile parameter $\eta = 1.5$).

Model	L_{11}	L_{12}	L_{21}	L_{22}	$|\tilde{n}/n|/|\tilde{T}/T|$ Near-field Mod	s/t	Far-field	$\chi_{\mathrm{eff}}^{\mathrm{HP}}/\chi_{\mathrm{eff}}^{\mathrm{PB}}$ Near-field Mod	s/t	Far-field
Collisionless neoclassical	1.04	−0.36	−1.40	1.65	0.19	1/1.5	1.66	1.59	1.42	2.63
Collisional neoclassical	0.33	0.06	−0.27	0.71	0.08	1/1.5	0.31	1.43	1.55	1.49
Anomalous DTE	2.0	6.0	1.0	15.0	0.14	1/1.5	0.47	0.14	21.2	4.56

4. Numerical modelling of generalized coupled transport

Although the analytical results presented above provide an insight into the coupling, it is necessary to solve the relevant equations numerically for the purposes of a quantitative comparison with experiment. The following equations were solved numerically:

$$\frac{\partial n_e}{\partial t} = \frac{1}{r}\frac{\partial}{\partial r}\left[rn_e\left(L_{11}\frac{n_e'}{n_e} + L_{12}\frac{T_e'}{T_e} - V_1\right)\right] + S(r,t) \tag{24}$$

$$\frac{3}{2}\frac{\partial(n_e T_e)}{\partial t} = \frac{1}{r}\frac{\partial}{\partial r}\left[rn_e T_e\left(L_{21}\frac{n_e'}{n_e} + L_{22}\frac{T_e'}{T_e} - \frac{3}{2}V_2\right) + \frac{5}{2}rn_e T_e\left(L_{11}\frac{n_e'}{n_e} + L_{12}\frac{T_e'}{T_e} - V_1\right)\right]$$
$$+ Q_\Omega(r,t) - Q_{exc}(r,t) - Q_{rad}(r,t) + Q_{ech}(r,t). \tag{25}$$

Here, L_{22} corresponds to the electron thermal diffusivity χ_e, L_{11} corresponds to the particle diffusivity D; the velocities V_1 and V_2 represent the non-diffusive terms and are negative for inward transport; S is the particle source, Q_Ω is the Ohmic heating source, Q_{exc} is the electron–ion exchange loss, Q_{rad} is the radiation loss and Q_{ech} is the ECRH source. The transport coefficients are, in general, functions of several plasma variables including gradients; the system of equations is then impossible to linearize or diagonalize. In the simplest case, however, an empirical radial dependence is assumed for all the diffusivities. Both the steady-state and perturbed parts of the density and temperature variables have to be considered. Approximate equilibrium profiles of density and temperature are used as initial conditions; the boundary conditions are

$$n_e'(0, t) = 0 \tag{26}$$

$$T_e'(0, t) = 0 \tag{27}$$

$$\Gamma(a, t) = -n_e\left(L_{11}\frac{n_e'}{n_e} + L_{12}\frac{T_e'}{T_e} - V_1\right)\Bigg|_{r=a} = F(t) \tag{28}$$

$$T_e'(a, t) = -AT_e(a, t). \tag{29}$$

The edge boundary conditions postulate a time-dependent particle flux (through which the effect of a modulated particle source may be introduced) and a Neumann-type cooling law and can be established from the density and temperature equilibrium profiles.

Ion energy transport has not been included in this analysis, because, at the relatively low densities and ion temperatures at which the modulation experiments on DITE were carried out, the steady-state and perturbed components of the energy transport through the ion channel are both small. The equipartition term is retained assuming a time-independent ion pressure equal to some fraction of the equilibrium electron pressure. Furthermore, the current density evolution is not included in the present analysis and a time-independent current distribution is assumed (this is consistent with the long magnetic field diffusion time of the order of 1 s).

The most difficult aspect of modelling perturbed coupled transport for given fluxes is the determination of the particle and energy source terms. It is clear that all the sources will be modulated, thus producing additional driving or damping terms. The perturbation of the Ohmic heating arises from the temperature dependence of the resistivity. The radiation loss and its perturbation are calculated using a radiation code based on bremsstrahlung and recombination radiation from the working gas and carbon and oxygen impurities

(Deliyanakis 1989); this calculates the power densities of the total radiation and the soft x-ray emission. The calculation of the particle source is more involved, because this depends on the distribution of neutral particles and on several atomic processes near the edge. The best assessment of the particle source is that provided by measurements of the Hα emission; this was measured and found to be modulated but it was impossible to obtain the absolute value of the particle source. Nevertheless, an effective particle source was calculated, as required to sustain the equilibrium density profile, and this was modulated with a relative amplitude and phase estimated from the observed modulation of the Hα emission.

The modulated, differential flux surface shifts are estimated on the basis of the large-aspect ratio; the underlying theory (Shafranov 1966) postulates horizontal shifts of the centres of the circular flux surfaces and these are modulated because of the electron pressure modulation. The horizontal, outward displacement of a flux surface of minor radius r, with respect to the centre of the outermost flux surface (minor radius a) is given by

$$\delta(r) = \int_r^a \frac{r'}{R_0}(\Lambda(r') + 1)\, dr' \tag{30}$$

with

$$\Lambda(r) = \left[\frac{1}{\pi r^2}\int_0^r \left(p(r') - p(r) + \frac{1}{2}\frac{B_\theta^2(r')}{2\mu_0}\right) 2\pi r'\, dr'\right] \Big/ \left(\frac{B_\theta^2(r)}{2\mu_0}\right) - 1 \tag{31}$$

p is the plasma pressure and B_θ is the (time-independent) poloidal field. In addition to the differential shifts considered above, a modulated, horizontal shift of the entire plasma column of comparable amplitude is present, since the response of the plasma column to the applied modulated power depends not only on the plasma equilibrium, but also on the response of the feedback stabilization system. For a complete description, the experimentally observed column shift is applied to the outermost flux surface.

A predictive transport code has been developed to implement this general model of coupled transport, with a view to evaluating various transport models in the context of modulated heating (Deliyanakis 1989). The perturbation in the coupled system is driven by a modulated ECRH power density term whose radial dependence is calculated by a ray-tracing code (Cox *et al* 1993). The solutions for the electron density and temperature profiles are advanced in time over several modulation cycles, subject to the generally varying transport coefficients and source terms. Equilibrium solutions for the electron density and temperature profiles are computed by allowing the system to evolve from the initial conditions without a perturbation, until the changes in the profiles become sufficiently small; this approach, however, usually fails to yield unique results, independent of the initial profiles, because of the accumulation of computational errors with nonlinear models. The local soft x-ray emissivity is calculated on the basis of the cut-off energy of the detection system. Simulated signals of line-integrated soft x-ray emissivity, electron cyclotron emission and line-integrated density are finally generated, taking the modulated flux surface shifts into account. Soft x-ray signals for both horizontal and vertical lines of sight are simulated, and their spatially varying amplitudes and phases are compared with the corresponding experimental data. The equilibrium solution provides a further assessment of the validity of the transport model.

5. Results from modelling generalized coupled transport

This section describes an application of the coupled transport model, whose purpose was to assess the compatibility of particle and energy fluxes containing finite off-diagonal

diffusivities with the analysed data from the modulated ECRH experiments on DITE (presented by Ashraf *et al* (1988), Cox *et al* (1993) and Deliyanakis (1989); some results of the present investigation were reported by Bishop *et al* (1989, 1990)). The investigation presented here was based on the simplest possible coupled transport model, that is one based on a time-independent diffusivity matrix with a single radial profile; particle and thermal pinch terms, with another radial profile, could be included. The diffusivity matrix used was that of the collisionless neoclassical model (for $Z_i = 1$, refer to Hinton and Hazeltine (1976) and section 3 of this paper); the diffusion matrix was naturally scaled to a level appropriate to anomalous transport and its radial variation was taken to be similar to that of the thermal diffusivity, as estimated by a power balance analysis. There is no justification in the use of this particular model of coupled transport, since neoclassical theory fails to predict even the level of the observed tokamak transport. Nevertheless, it provides one with a means of testing the basic aspects of coupled transport: the analytical solutions above indicate a finite density modulation on the one hand, and a discrepancy between the equilibrium and dynamical values of the effective thermal diffusivity on the other hand.

The practical aspects of the application of the diffusive thermal transport model to the results of the DITE modulation experiments (Cox *et al* 1993, Deliyanakis 1989) are also pertinent to the application of the present coupled transport model; several of the considerations that were regarded there, in particular the density and temperature profiles, are more important in this case. The equilibrium profiles were established from a combination of experimental observations (mainly of the temperature profile using the ECE diagnostic) and results from the equilibrium section of the transport code. As the soft x-ray (SXR) data provide the most extensive information from the DITE modulation experiments, the dependence of the SXR emissivity on both electron temperature and electron density is an important aspect of the model. This highlights the importance of the SXR modulation indices for both temperature and density; these depend on the impurity content and confinement. The temperature dependence was calculated by the radiation code, but the modulation index for the density dependence was fixed at 2 (this was the natural choice, but the real value could be nearer 1).

The complexity of the present model means that the experimental uncertainties are compounded by computational uncertainties, particularly so when the transport model involves sensitive dependences on the varying plasma parameters. It was therefore impossible conclusively to ascertain the validity or otherwise of a given transport model, using the present experimental data (Deliyanakis 1989, Bishop *et al* 1989, 1990), and only qualitative significance should be ascribed to the tentative results that were obtained from that analysis.

A typical comparison of the coupled diffusion model with the modulation data from a medium-density discharge ($\bar{n}_e = 1.6\times10^{-19}$ m^{-3}, $I_p = 100$ kA, $B_\phi = 2$ T) with fundamental, off-axis heating (100 kW at 60 GHz, with a modulation period of 7 ms) is presented in figures 1 and 2, showing the SXR and ECE data respectively; the modulation amplitudes and the relative phases of the experimental and the simulated data are shown, in addition to the average (equilibrium) levels and the relative modulation levels. The corresponding modulation data for the simulated, line-integrated density signals are shown in figure 3; unfortunately, the poor quality of the density modulation data does not allow a detailed comparison of the profiles to be made. For this case, figures 4 and 5 show the profile evolution of the perturbed components of the electron density and temperature, respectively. The main conclusions from this exercise are as follows.

(i) The off-diagonal transport coefficients can be comparable in magnitude to the diagonal ones, without necessarily leading to a large density modulation; in the case with
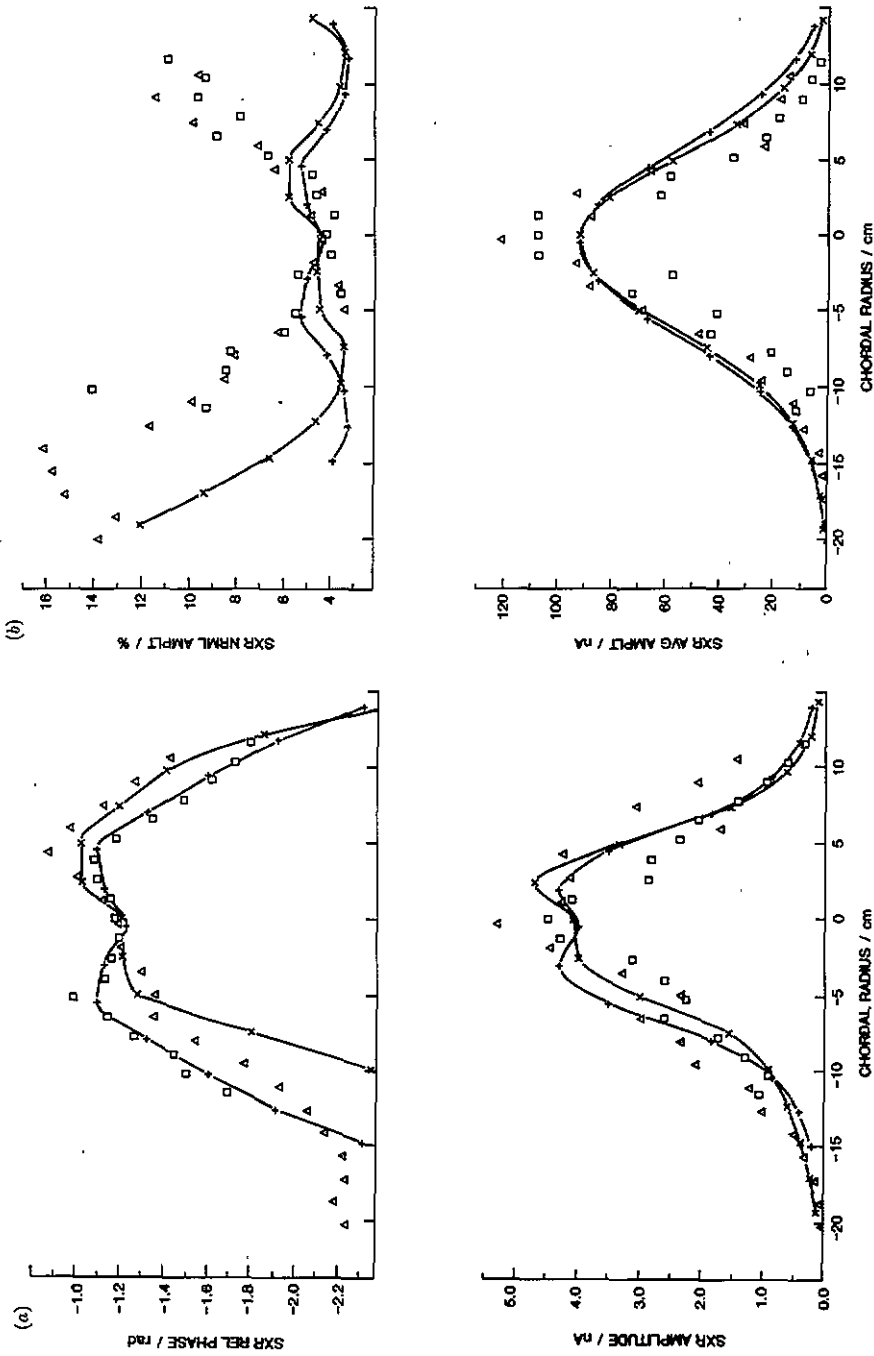
Figure 1. Experimental SXR data ((a) relative phase and modulation amplitude; (b) percentage modulation and equilibrium level), fitted with coupled transport model: H discharge (33855), medium density, fundamental off-axis ECRH, modulated at 143 Hz. Experimental data from the horizontal (squares) and vertical (triangles) SXR arrays are shown; both sets of data are simulated by the model (+ and x, respectively).
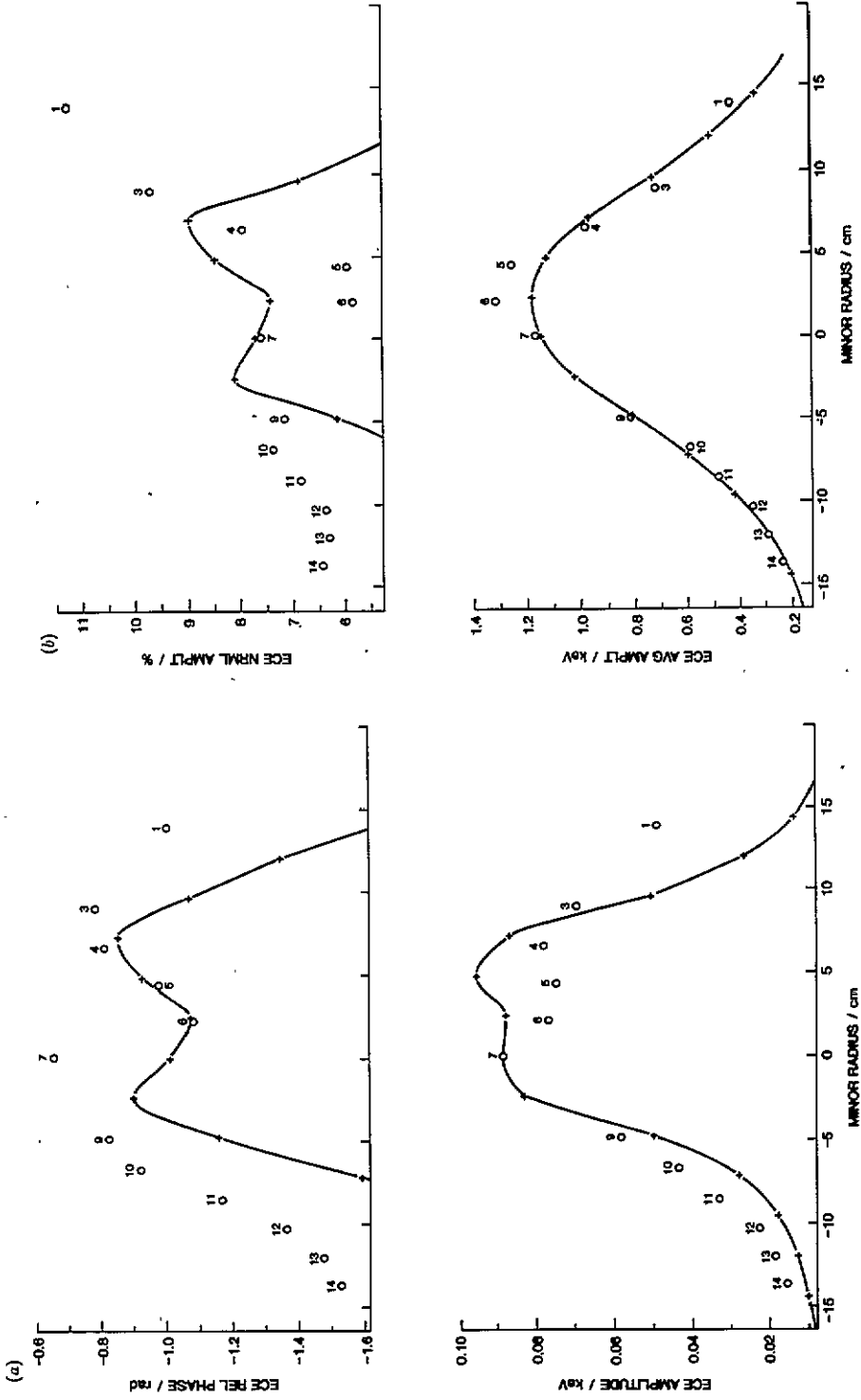
Figure 2. Experimental ECE data ((a) relative phase and modulation amplitude; (b) percentage modulation and equilibrium level), fitted with coupled transport model: discharge of figure 1. Experimental data from the 14 ECE channels are shown (circles). The ECRH power deposition is centred at 4 cm with a FWHM of 3 cm.
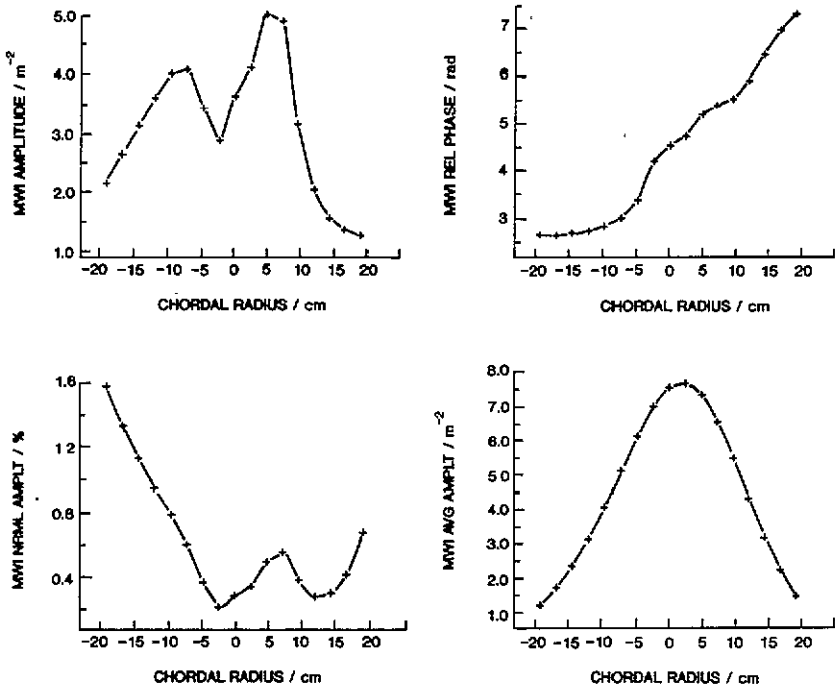
Figure 3. Line-integrated density modulation data (modulation amplitude, relative phase, percentage modulation and equilibrium level) as simulated: model of figures 1–2.
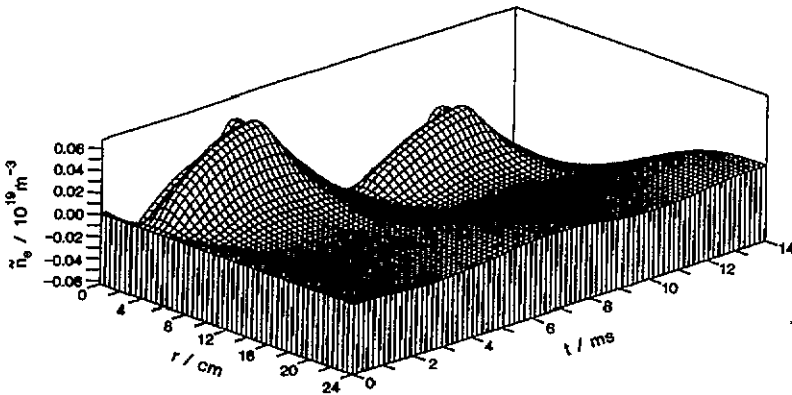

Figure 4. Electron density perturbation $\tilde{n}_e$ plotted as a function of minor radius r and time t, over two modulation cycles: model of figures 1–2.

on-axis heating, the modulation levels of central density and temperature were 3% and 15% respectively. The behaviour of the coupled transport model is sensitive to the choice of diffusivity matrix: whilst the diffusivity matrix used in the present analysis did not lead to good agreement with all the experimental data, it appears likely that a different matrix could yield results in closer agreement. The effective power balance thermal diffusivity (0.9 m^2 s^{-1} at the radius $a/3$), as calculated from the code profiles and energy sources, was in good agreement with the corresponding experimental value.
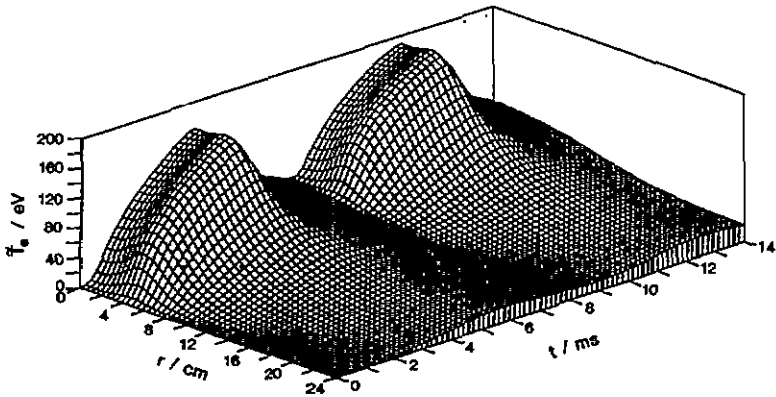
Figure 5. Electron temperature perturbation $\tilde{T}_e$ plotted as function of minor radius r and time t, over two modulation cycles: model of figures 1–2.

(ii) The computed temperature perturbation was similar, in form and magnitude, to that obtained from the simpler diffusive thermal transport analysis (described by Cox *et al* (1993) and Deliyanakis (1989)).

(iii) The computed local density perturbation due to the transport coupling was small under some conditions, in particular with off-axis heating, and its scale-length was shorter than that of the temperature perturbation. The shorter scale-lengths led to a significant cancellation of the modulation amplitude on calculating the line-integrated values; in a case with on-axis heating, the modulation level of the local density was about 3% at the centre, but that of the line-integrated signal was $\lesssim 1\%$, increasing towards the edge; in a case with off-axis heating, the modulation levels were lower and the cancellation was still significant. The model results were therefore fully consistent with the low values of the measured relative modulation levels of the line-integrated density signals (Cox *et al* 1993, Deliyanakis 1989); the associated relative phases and their profiles could not be compared, as the phase of the density perturbations could not be reliably determined from the microwave interferometer data.

(iv) The measured density modulation levels could *not* be interpreted in the absence of a local density modulation, that is from the horizontal plasma motion alone. Furthermore, only the presence of coupled transport can explain the observed initial *decrease* in the density on *all* chords at the time when the positive energy perturbation is applied (cf figures 4 and 5): the perturbation of the particle source would lead to a positive density perturbation, and the horizontal plasma motion would lead to apparent density perturbations of both signs.

(v) Good agreement was obtained in fitting the computed temperature and SXR emissivity responses to those measured experimentally. However, the agreement is less satisfactory than that obtained from a simple diffusive thermal transport model, as described by Cox *et al* (1993). It was found that, under the present conditions, the modulation of temperature still had a dominant effect on that of the line-integrated SXR emissivity (only a small change in the predicted SXR modulation data was observed when the density modulation was eliminated from the calculation).

(vi) As expected, the inclusion of a modulated particle source plays an important role in determining the level as well as the precise spatial variation of the density modulation. As the particle source perturbation was included using an empirical amplitude and phase (inferred from the observed modulation of the Hα emission), this aspect of the present model is a major source of uncertainty.

(vii) The explicit inclusion of a pinch term in both particle and thermal fluxes led to a small modification of the modulation results, because of the finite density modulation: the phase gradients became somewhat larger, for the same diffusivity values.

(viii) The modulation of the MHD shifts of the flux surfaces led to the expected asymmetries, the results being consistent both with the experimental shifts, as measured with the magnetic diagnostics, and with the experimental modulation data. A column shift was applied, with an appropriate amplitude (about 1 mm) and phase; this led to a close agreement with the signals from the vertical SXR chords.

(ix) All the results of the coupled transport model were strongly dependent on the equilibrium profiles of density and temperature, as well as on the form of the transport model. The experimental temperature profile that was used was found to be within an average deviation of 10% from that obtained by allowing the model solution to approach energy equilibrium with the calculated energy sources. As a suitable calculation of the particle source was not implemented, such a test could not be carried out on the density profile.

The main weaknesses of this analysis are (a) the use of an effective particle source, as described in the previous section, with a roughly estimated modulated component; and (b) the use of parameter-independent diffusivities, contrary to the predictions of most transport theories.

6. Conclusions

A model of coupled particle and energy transport has been used in conjunction with ECRH modulation data from DITE, its main purpose being to shed light upon the causes and effects of the observed density modulation and to demonstrate the usefulness of predictive modelling for the assessment of transport models. Realistic assessments of the energy sources and of the flux surface shifts have been carried out and several different coupled transport models have been investigated. Good qualitative agreement of coupled transport models with experimental data has been obtained and all the features of these data have been reproduced; the possibility of coupled transport has become evident. The main conclusion of this exercise is that transport matrices with relatively large off-diagonal components can lead to small apparent density modulation and hence produce results consistent with experimental observations from modulation experiments, such as those on DITE. At the same time such matrices affect the propagation of the thermal wave, resulting in modified effective heat diffusivities. Whilst it has not been possible conclusively to establish the nature of the underlying transport mechanisms, it has been shown that some forms of coupling are consistent with experimental data; however, some models, such as the dissipative-trapped-electron mode, produce extreme results which are incompatible with the experimental data and can therefore be ruled out.

It has been demonstrated that modulated heating, possibly combined with equilibrium measurements and alternative perturbations of the equilibrium, affords one with a powerful technique for ascertaining the validity or otherwise of proposed transport models, subject to some developments in the experiment: the technique is especially powerful if (a) the ECRH power has a strongly localized deposition and (b) measurements of the temperature and density perturbations are available with good spatial resolution. The density and temperature gradients of both the electron and ion components are of particular importance in connection with transport models; in general, it is important to include the ion energy balance in the analysis. This work also highlights the importance of employing different

methods of perturbation on similar discharges: such methods include modulation of heating power, modulation of gas feed, pellet injection and the naturally excited sawtooth pulse. Perturbation experiments would yield maximum information if carried out under varied conditions; in particular the variation of the steady-state input power (ohmic, ECRH or other) should modify the profiles and the transport, and can possibly reveal some of the dependences of the particle and thermal fluxes on the plasma parameters, when such fluxes are measured by both equilibrium and dynamical methods. Furthermore, the point of application of some perturbations can be varied, thus providing information about both the outward and inward propagation.

The relevance of, and need for, *predictive* transport codes for the assessment of complex transport models, in particular those with strongly nonlinear fluxes, is evident from this work. Although dynamical transport matrices can be obtained from perturbation data (e.g., O'Rourke *et al* 1992), it is difficult to determine the steady-state matrices and their functional dependence from a direct interpretation. Whilst direct interpretation of experimental data (e.g., de Haas *et al* 1991, Moret *et al* 1992) is more convenient and apparently conclusive, it is only predictive interpretation that can account for all possible complications and afford one with a potentially conclusive way of validating proposed transport models. The complications that limit the applicability of direct approaches are (a) nonlinear fluxes, (b) large perturbations and (c) non-stationary conditions. On the other hand, the predictive approach is dependent on, and limited by, the availability of detailed source terms (leading to uncertainties smaller than the discrepancies between contending transport models).

References

Ashraf M *et al* 1988 *Proc. 12th IAEA Conf. on Plasma Physics and Controlled Nuclear Fusion Research (Nice)* vol 1, p 275

Bishop C M and Connor J W 1990 *Plasma Phys. Control. Fusion* **32** 203

Bishop C M *et al* 1989 *Proc. 16th EPS Conf. on Controlled Fusion and Plasma Physics (Venice)* 13B, vol 3, p 1131

Bishop C M *et al* 1990 *Proc. 17th EPS Conf. on Controlled Fusion and Plasma Physics (Amsterdam)* 14B, vol 1, p 178

Cox M *et al* 1993 *Nucl. Fusion* **33** 1657

Deliyanakis N 1989 A study of tokamak energy and particle transport, based on modulated electron cyclotron resonance heating *DPhil. Thesis* University of Oxford

Fredrickson E D *et al* 1986 *Nucl. Fusion* **26** 849

Gambier D J *et al* 1990 *Nucl. Fusion* **30** 23

Gentle K W 1988 *Phys. Fluids* **31** 1105

de Haas J C M *et al* 1991 *Nucl. Fusion* **31** 1261

Hinton F L and Hazeltine R D 1976 *Rev. Mod. Phys.* **48** 239

Horton W 1976 *Phys. Fluids* **19** 711

Hossain M *et al* 1987 *Phys. Rev. Lett.* **58** 487

Jahns G L *et al* 1986 *Nucl. Fusion* **26** 226

Moret J-M *et al* 1992 *Nucl. Fusion* **32** 1241

O'Rourke J 1993 *Plasma Phys. Control. Fusion* **35** 111

O'Rourke J, Rimini F G and Start D F H 1992 *Nucl. Fusion* **32** 1861

Shafranov V D 1966 *Reviews of Plasma Physics* vol 2, ed M A Leontovich (New York: Consultants Bureau) p 103

Tubbing B J D, Lopes Cardozo N J and van der Wiel M J 1987 *Nucl. Fusion* **27** 1843